A. Caffagni

D. Angeli[1]
e-mail: diego.angeli@unimore.it

G. S. Barozzi

DIEF - Dipartimento di Ingegneria "Enzo Ferrari",
Università di Modena e Reggio Emilia,
Via Vignolese, 905,
41125 Modena, Italy

S. Polidoro
Dipartimento di Scienze Fisiche,
Informatiche e Matematiche,
Università di Modena e Reggio Emilia,
Via G. Campi, 213/b,
41125 Modena, Italy

A Revised Approach for One-Dimensional Time-Dependent Heat Conduction in a Slab

Classical Green's and Duhamel's integral formulas are enforced for the solution of one dimensional heat conduction in a slab, under general boundary conditions of the first kind. Two alternative numerical approximations are proposed, both characterized by fast convergent behavior. We first consider caloric functions with arbitrary piecewise continuous boundary conditions, and show that standard solutions based on Fourier series do not converge uniformly on the domain. Here, uniform convergence is achieved by integrations by parts. An alternative approach based on the Laplace transform is also presented, and this is shown to have an excellent convergence rate also when discontinuities are present at the boundaries. In both cases, numerical experiments illustrate the improvement of the convergence rate with respect to standard methods.
[DOI: 10.1115/1.4007982]

Keywords: heat equation, semi-analytical numerical methods, Fourier series, Green's functions, Duhamel's integrals

1 Introduction

Due to its one-dimensional character, heat conduction in a slab is a typical introductory case to heat transfer theory. Besides its mathematical interest, the case has practical importance for two main reasons. First, a one-dimensional feature is in many cases a good approximation to real conditions of two- and three-dimensional heat flow in structures and, second, analytical solutions to the one-dimensional heat equation are easily found, and they form a very valuable basis for the benchmarking of multidimensional numerical approaches. For these reasons, heat conduction in slabs has been studied along the last century for either steady or unsteady conditions, and under a variety of thermal boundary and initial conditions [1–4].

The basic case is described as follows: two opposite faces of a slab are kept at uniform temperatures T_1 and T_2, while the peripheral contour of the slab is adiabatic. Adding the assumptions of homogeneous and isotropic material, the temperature T within the wall only varies with the coordinate x normal to the active boundaries, and possibly with time; the thermal problem is therefore one-dimensional in space. In the absence of internal heat generation and for constant properties, the steady-state temperature distribution within the slab for fixed values of T_1 and T_2 is readily found to be linear.

Several analytical methods have been proposed and used so far to tackle the time-dependent one-dimensional heat equation. As summarized in Ref. [5], these include the separation of variables, the use of Laplace transforms, the modeling by sources and sinks, the method of images, and the Duhamel's method. Among those, the method of separation of variables has been the most widely adopted to investigate transient 1D heat conduction in slabs [6]. We refer to Refs. [7,8] and to the bibliography therein for a survey on the recent literature on this subject. Very recently, semi-analytical methods were also employed to solve steady-state 1D conduction at the nanoscale [9], and 2D transient conduction between two parallel, isothermal cylinders in an infinite medium [10].

It is noteworthy that Eq. (1) is analogous to the Couette problem, which is a simplified Navier–Stokes equation governing the flow of a fluid between two parallel plates moving at different velocities. Provided that the fluid is constant-property and Newtonian, no axial pressure gradient is imposed, and advective acceleration terms are overlooked, the governing equation for this class of fluid-dynamic problems coincides with Eq. (3) when appropriate nondimensional terms are used. The solutions provided here therefore hold for both the general 1D heat conduction and the Couette problems.

In this paper, classical Green's representation formulas for time-dependent heat diffusion in a slab are revised. General, possibly discontinuous, Dirichlet's boundary conditions are considered where no limitation is imposed to the shape of the functions describing either the initial temperature distribution within the system or the time-dependent boundary values.

Following standard solution procedures [1] a series expansion of the Green's function is first obtained by the Duhamel's method. Since only continuous functions appear in this series, it cannot converge uniformly on the domain to a discontinuous function. This implies that the accuracy of the solution deteriorates when a numerical approximation of such series is calculated. When the boundary data are more regular, twice differentiable for instance, we achieve the uniform convergence by using a double integration by parts. The rate of convergence is seen to be higher when considering smooth boundary conditions, while it slows down in the presence of discontinuities at the boundaries.

The theoretical and numerical study is also carried out for a second method, based on the Laplace transform [5]. In this case, the improvement is demonstrated to be independent of the regularity of the boundary data. On the contrary, we get a good rate of convergence also for discontinuous boundary conditions. From the theoretical point of view, this issue depends on the fact that the first term in the series expansion may be discontinuous at the boundary, so that the discontinuities of the boundary data do not prevent the fast convergence of the series.

For the sake of validation, the transient due to an exponential-law change in one of the boundary values is considered. A further numerical example is provided as well, including a general initial

[1]Corresponding author.
Contributed by the Heat Transfer Division of ASME for publication in the Journal of Heat Transfer. Manuscript received April 16, 2012; final manuscript received October 23, 2012; published online February 14, 2013. Assoc. Editor: Giulio Lorenzini.

temperature distribution within the slab, and the imposition of two time-varying temperatures at the slab extremities.

2 Statement of the Problem

The physical problem to be examined is sketched in Fig. 1. Along the x axis we assume to have a slab, whose material is homogeneous and isotropic, and whose thermal diffusivity α, is constant. An initial temperature distribution T_0 is prescribed at each point of the slab, and the boundary temperature values vary with time following the given general laws $T_1(t)$ and $T_2(t)$. According to Fourier's law, the one-dimensional heat equation without internal heat source writes

$$\frac{\partial T}{\partial t} = \alpha \frac{\partial^2 T}{\partial x^2} \tag{1}$$

where t denotes time $(0 < t < \infty)$, x is the space variable $(0 \leq x \leq L)$, and L is the slab length. When coupled with the following boundary and initial conditions:

$$\begin{aligned} T(x,0) &= T_0(x), \quad 0 \leq x \leq L \\ T(0,t) &= T_1(t), \quad t \geq 0 \\ T(L,t) &= T_2(t), \quad t \geq 0 \end{aligned} \tag{2}$$

Equation (1) has a unique solution. Here T_0, T_1, and T_2 are given bounded continuous functions of their arguments, with $T_0(0) = T_1(0)$ and $T_0(L) = T_2(0)$. We recall that T satisfies the maximum principle: if we let

$$T_{\min}(s) = \min\left\{\min_{[0,L]} T_0,\ \min_{[0,s]} T_1,\ \min_{[0,s]} T_2\right\}$$

$$T_{\max}(s) = \max\left\{\max_{[0,L]} T_0,\ \max_{[0,s]} T_1,\ \max_{[0,s]} T_2\right\}$$

for every positive s, we have $T_{\min}(s) \leq T(x,t) \leq T_{\max}(s)$, for all $(x,t) \in [0,L] \times [0,s]$. Setting $T_{\min} = \inf_{s>0} T_{\min}(s)$ and $T_{\max}(s) = \sup_{s>0} T_{\max}(s)$, we recast Eqs. (1) and (2) by using the following dimensionless coordinates and unknown:

$$z := \frac{x}{L}, \quad \tau := \frac{t\alpha}{L^2}, \quad \vartheta(z,\tau) := \frac{T(x,t) - T_{\min}}{T_{\max} - T_{\min}}$$

In heat transfer literature, τ is also called the Fourier number. Using the above changes, the governing equation can be written in the form

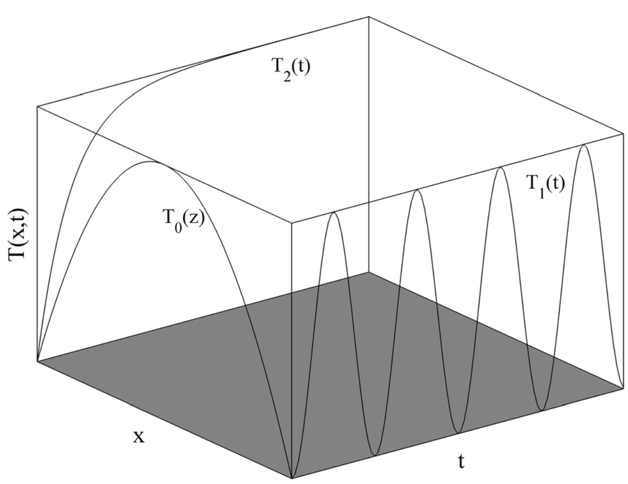

Fig. 1 Schematic diagram of the problem

$$\frac{\partial \vartheta}{\partial \tau} = \frac{\partial^2 \vartheta}{\partial z^2} \quad (z,\tau) \in]0,1[\times]0,\infty[\tag{3}$$

with

$$\begin{aligned} \vartheta(z,0) &= \psi(z) := \frac{T_0(Lz) - T_{\min}}{T_{\max} - T_{\min}}, \quad 0 \leq z \leq 1 \\ \vartheta(0,\tau) &= \varphi_1(\tau) := \frac{T_1(\omega\tau) - T_{\min}}{T_{\max} - T_{\min}}, \quad \tau \geq 0 \\ \vartheta(1,\tau) &= \varphi_2(\tau) := \frac{T_2(\omega\tau) - T_{\min}}{T_{\max} - T_{\min}}, \quad \tau \geq 0 \end{aligned} \tag{4}$$

We finally note that $0 \leq \vartheta(z,\tau) \leq 1$ for all $(z,\tau) \in]0,1[\times]0,+\infty[$, by the maximum principle.

3 The Standard Approach

In this section we recall a well-known solution to problem (3)–(4), based on Green representation formulas [1]. A Green's function is an integral kernel G that gives the solution of a partial differential equation with Dirichlet boundary conditions. In our case, the representation formula reads as follows:

$$\begin{aligned} \vartheta(z,\tau) = &\int_0^1 G((z,\tau),(y,0))\psi(y)dy + \int_0^\tau G((z,\tau),(0,\lambda))\varphi_1(\lambda)d\lambda \\ &+ \int_0^\tau G((z,\tau)(1,\lambda))\varphi_2(\lambda)d\lambda \end{aligned} \tag{5}$$

The solution approach consists in deriving a series expansion for the Green's function G. Such series, provided that it satisfies some convergence properties, can then be used to obtain a numerical solution of the Dirichlet problem.

We start by splitting, without any loss of generality, problem (3)–(4) into three subproblems

$$\vartheta(z,\tau) = \eta(z,\tau) + \xi(z,\tau) + \chi(z,\tau) - (1-z)\psi(0) - z\psi(1) \tag{6}$$

where

$$\begin{aligned} &\frac{\partial \eta}{\partial \tau} = \frac{\partial^2 \eta}{\partial z^2} \quad (z,\tau) \in]0,1[\times]0,\infty[\\ &\eta(z,0) = \psi(z) - \psi(0) - z\psi(1), \quad \eta(0,\tau) = 0, \quad \eta(1,\tau) = 0 \end{aligned} \tag{7}$$

$$\begin{aligned} &\frac{\partial \xi}{\partial \tau} = \frac{\partial^2 \xi}{\partial z^2} \quad (z,\tau) \in]0,1[\times]0,\infty[\\ &\xi(z,0) = 0, \quad \xi(0,\tau) = \varphi_1(\tau) - \varphi_1(0), \quad \xi(1,\tau) = 0 \end{aligned} \tag{8}$$

and

$$\begin{aligned} &\frac{\partial \chi}{\partial \tau} = \frac{\partial^2 \chi}{\partial z^2} \quad (z,\tau) \in]0,1[\times]0,\infty[\\ &\chi(z,0) = 0, \quad \chi(0,\tau) = 0, \quad \chi(1,\tau) = \varphi_2(\tau) - \varphi_2(0) \end{aligned} \tag{9}$$

It is not restrictive to assume that $\psi(0) = \varphi_1(0) = 0$ and $\psi(1) = \varphi_2(0) = 0$.

3.1 Solution to Subproblem (7). Let us consider first problem (7). Following the method introduced by Fourier [1], we look for solutions in the form $\eta(z,\tau) = f(z)h(\tau)$, and rely on the superposition principle. We find

$$\eta(z,\tau) = \sum_{n=1}^{\infty} a_n e^{-n^2\pi^2\tau} \sin(n\pi z), \quad a_n = 2\int_0^1 \sin(n\pi y)\psi(y)dy \tag{10}$$

If we assume that the initial condition ψ is smooth enough, say differentiable with continuous derivative ψ', then the series (10) converges uniformly on the whole domain.

If we consider a merely continuous, or possibly discontinuous, initial condition ψ, we have a weaker convergence near $\tau = 0$ (see, for instance, Di Benedetto [11], Secs. 6 and 10 in Chapter 5). More specifically, if ψ belongs to $L^2([0,1])$, the series (10) is uniformly convergent in the set $[0,1] \times [\varepsilon, +\infty[$ for any positive ε. Indeed, we have

$$\sum_{n=1}^{\infty} |a_n|^2 \leq 2 \parallel \psi \parallel^2_{L^2([0,1])} \tag{11}$$

so that

$$\sup_{[0,1]\times[\varepsilon,+\infty[} \left| a_n e^{-n^2\pi^2\tau} \sin(n\pi z) \right| \leq \sqrt{2} e^{-n^2\pi^2\varepsilon} \parallel \psi \parallel_{L^2([0,1])}$$

for every n. Since $\sum_{n=1}^{\infty} e^{-n^2\pi^2\varepsilon}$ converges, we have that series (10) is uniformly convergent. It is also known that η takes the initial data in the $L^2([0,1])$ sense, i.e.,

$$\lim_{\tau\to 0} \parallel \eta(\cdot,\tau) - \psi \parallel_{L^2([0,1])} = 0 \tag{12}$$

Moreover, from Eq. (11) we also get the following stability estimate:

$$\parallel \eta_N \parallel_{L^2([0,1]\times[0,T])} \leq \sqrt{\frac{T}{2}\sum_{n=1}^{\infty} a_n^2} = \sqrt{T} \parallel \psi \parallel_{L^2([0,1])} \tag{13}$$

for any positive integer N, where

$$\eta_N(z,\tau) = \sum_{n=1}^{N} a_n e^{-n^2\pi^2\tau} \sin(n\pi z)$$

We finally note that the regularity of the initial condition ψ, improves the convergence of the series (10). For instance, if ψ' belongs to $L^2([0,1])$, then

$$\sum_{n=1}^{\infty} |a_n| \leq c_0 \parallel \psi' \parallel_{L^2([0,1])} \tag{14}$$

for some universal positive constant c_0. Equation (14) is a proof of both stability and uniform convergence of Eq. (10).

3.2 Solution to Subproblems (8) and (9). The standard approach to problem (8) is based on the Duhamel's integral. Assuming $\varphi_1(0) = 0$, the solution reads

$$\xi(z,\tau) = \int_0^{\tau} \left[\varphi_1(\lambda) \frac{\partial F_1(z,\tau-\lambda)}{\partial \tau} \right] d\lambda \tag{15}$$

where F_1 satisfies

$$\frac{\partial F_1}{\partial \tau} = \frac{\partial^2 F_1}{\partial z^2}, \quad (z,\tau) \in]0,1[\times]0,\infty[$$

$$F_1(z,0) = 0, \quad F_1(0,\tau) = 1, \quad F_1(1,\tau) = 0 \tag{16}$$

Note that Eq. (15) provides us with the Green's function

$$G((z,t),(0,\lambda)) = \frac{\partial F_1(z,\tau-\lambda)}{\partial \tau}$$

and that F_1 is discontinuous at (0, 0).

Problem (16) can be further redefined by putting $F_1(z,\tau) = 1 - z + \rho(z,\tau)$, where ρ is the solution of

$$\frac{\partial \rho}{\partial \tau} = \frac{\partial^2 \rho}{\partial z^2} \quad (z,\tau) \in]0,1[\times]0,\infty[$$

$$\rho(0,\tau) = 0, \quad \rho(1,\tau) = 0, \quad \text{for} \quad \tau \geq 0$$

$$\rho(z,0) = z - 1, \quad \text{for} \quad 0 < z < 1 \tag{17}$$

Problem (17) is analogous to problem (7), except for the jump of the initial condition at $z=0$. Since $\rho(z,0)$ belongs to $L^2([0,1])$, the series (10) gives a solution of the above problem which takes the initial condition in the $L^2([0,1])$ sense. By computing the Fourier coefficients of $(1 - z)$ we find

$$F_1(z,\tau-\lambda) = 1 - z - \frac{2}{\pi}\sum_{n=1}^{\infty}\frac{1}{n} e^{-n^2\pi^2(\tau-\lambda)} \sin(n\pi z) \tag{18}$$

From the above equation and Eq. (15) we get the solution of Eq. (8) in the following form:

$$\xi(z,\tau) = 2\pi \int_0^{\tau} \sum_{n=1}^{\infty} n e^{-n^2\pi^2(\tau-\lambda)} \sin(n\pi z) \varphi_1(\lambda) d\lambda \tag{19}$$

Analogously, the solution χ to problem (9) writes

$$\chi(z,\tau) = \int_0^{\tau} \left[\varphi_2(\lambda) \frac{\partial F_2(z,\tau-\lambda)}{\partial \tau} \right] d\lambda \tag{20}$$

where $F_2(z,\tau) = F_1(1-z,\tau)$, with $F_2(z,0) = 0, F_2(0,\tau) = 0$, and $F_2(1,\tau) = 1$. In light of the above considerations, we can write

$$\chi(z,\tau) = 2\pi \int_0^{\tau} \sum_{n=1}^{\infty} n e^{-n^2\pi^2(\tau-\lambda)} \sin(n\pi z)(-1)^{n+1} \varphi_2(\lambda) d\lambda \tag{21}$$

3.3 Convergence Properties. In view of Eqs. (10), (19), and (21), it is natural to seek the solution ϑ of Eq. (3) as $\vartheta(z,\tau) = \lim_{N\to\infty} \vartheta_N(z,\tau)$, where $\vartheta_N = \xi_N + \eta_N + \chi_N$, with

$$\xi_N(z,\tau) = 2\pi \int_0^{\tau} \sum_{n=1}^{N} n e^{-n^2\pi^2(\tau-\lambda)} \sin(n\pi z) \varphi_1(\lambda) d\lambda$$

$$\chi_N(z,\tau) = 2\pi \int_0^{\tau} \sum_{n=1}^{N} n e^{-n^2\pi^2(\tau-\lambda)} \sin(n\pi z)(-1)^{n+1} \varphi_2(\lambda) d\lambda$$

$$\eta_N(z,\tau) = 2\sum_{n=1}^{N} e^{-n^2\pi^2\tau} \sin(n\pi z) \int_0^1 \psi(y) \sin(n\pi y) dy \tag{22}$$

However, $\xi_N \to \xi$ as $N \to \infty$ if and only if

$$\int_0^{\tau} \sum_{n=1}^{\infty} n e^{-n^2\pi^2(\tau-\lambda)} \sin(n\pi z) \varphi_1(\lambda) d\lambda = \sum_{n=1}^{\infty} \int_0^{\tau} n e^{-n^2\pi^2(\tau-\lambda)} \sin(n\pi z) \varphi_1(\lambda) d\lambda \tag{23}$$

The same remark also applies to χ_N.

Since the uniform convergence of the series (19) and (21) is a sufficient condition for interchanging integration and summation, some remarks about their convergence properties are in order. When discussing Eq. (14), we already noticed that the regularity of the initial condition ψ improves the convergence of the series (10). However, this is not the case for Eqs. (19) and (21), even if the boundary conditions φ_1 and φ_2 are smooth. As an example, let

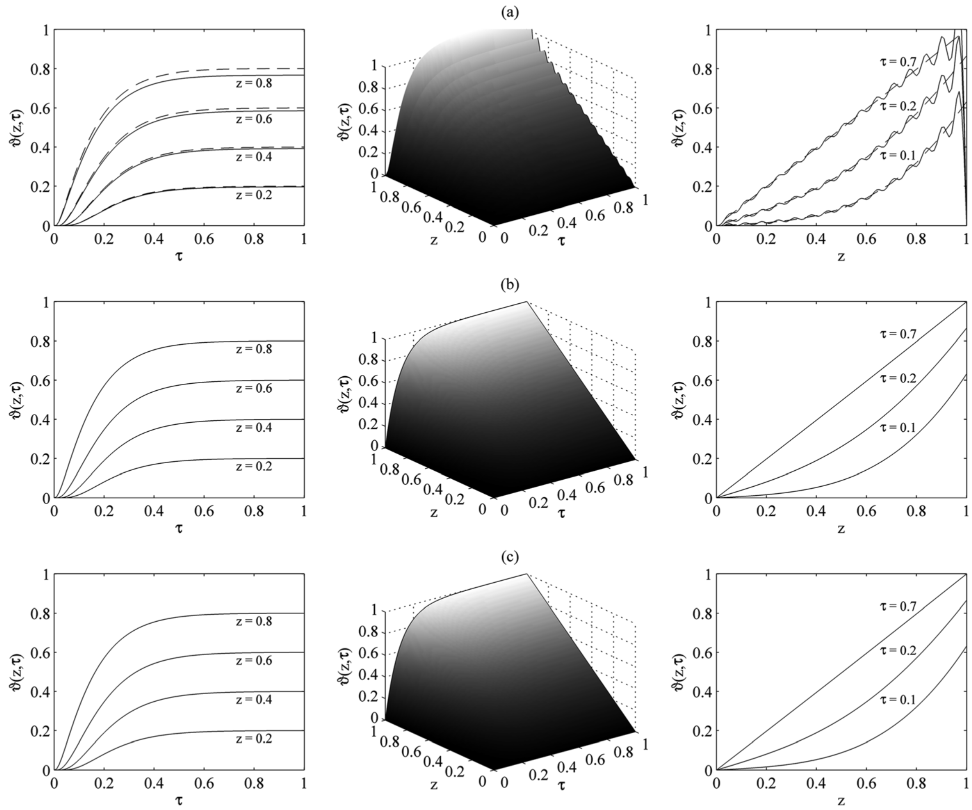

Fig. 2 Solutions to Eq. (3) with boundary conditions (24), computed on the $[0,1]\times[0,1]$ domain, according to: (*a*) Eq. (22); (*b*) Eq. (29); (*c*) Eq. (36). All the finite sums are evaluated up to a number of terms $N = 30$. Left panels: profiles of $\vartheta(z,\tau)$ for selected *z*-values. Middle panels: surface visualization of $\vartheta(z,\tau)$. Right panels: profiles of $\vartheta(z,\tau)$ for selected τ-values. Dashed lines in left and right panels denote a numerical solution obtained by second-order finite differencing.

us consider problem (3) with Eq. (24) (as defined in the next paragraph), and define $f_n(z,\tau)$ as

$$f_n(z,\tau) = n\sin(n\pi z)\int_0^\tau e^{n^2\pi^2(\lambda-\tau)}\varphi_2(\lambda)d\lambda$$

We have that

$$\sup_{[0,1]\times[\tau_0,+\infty[}|f_n(z,\tau)| = n\int_0^\tau e^{n^2\pi^2(\lambda-\tau)}\varphi_2(\lambda)d\lambda \geq$$
$$n\left(1-e^{-10\tau_0}\right)\int_0^\tau e^{n^2\pi^2(\lambda-\tau)}d\lambda \geq \frac{1}{\pi^2 n}\left(1-e^{-10\tau_0}\right)\left(1-e^{-n^2\pi^2\tau_0}\right)$$

for every n, so that $\sum_{n=1}^\infty \sup|f_n|$ diverges.

3.4 Numerical Test. The unsatisfactory convergence of series (19) and (21) can be easily demonstrated by the following simple numerical test, where the initial-boundary value problem (3) is considered with:

$$\begin{aligned}
&\vartheta(z,0) = \psi(z) := 0, && 0 \leq z \leq 1\\
&\vartheta(0,\tau) = \varphi_1(\tau) := 0, && \tau \geq 0\\
&\vartheta(0,\tau) = \varphi_2(\tau) := 1-e^{-10\tau}, && \tau \geq 0
\end{aligned} \qquad (24)$$

Figure 2(*a*) portrays a surface plot of the solution for $(z,\tau)\in[0,1]\times[0,1]$, alongside with contour lines for selected values of z and τ. The finite sums in Eq. (22) have been evaluated with $N = 30$ terms, integrals having been computed by adaptive Lobatto quadrature methods. A finite-difference solution of problem (3) with conditions (24) has also been computed and displayed for reference in the left and right panels of Fig. 2(*a*). Explicit Euler and second-order central differences schemes have been adopted for the time and spatial derivative, respectively, and constant time and spatial steps have been used, namely $\Delta\tau = 0.005$ and $\Delta z = 0.1$.

The comparison clearly points out the poor convergence of the series. Indeed, the maximum principle states that the maxima of *analytical* solutions of the heat equation necessarily lie on the boundary of the domain. This principle is evidently not respected by solution (22): in fact, the plots in Fig. 2(*a*) reveal the appearance of a *Gibbs phenomenon*, which typically occurs when considering the Fourier series of a discontinuous function.

4 Improving Convergence of the Standard Approach

Stemming from the standard approach, we will now propose an improved solution to problem (3)–(4), based on a simple integration by parts [12].

Considering Eq. (15) first, we recall that F_1 is continuous at every point $(z,\tau)\in[0,1]\times[0,+\infty[$, with $(z,\tau)\neq(0,0)$. In addition, we observe that, for every $z\in]0,1[$, the derivative of the series (19) converges uniformly for $\lambda\in]\varepsilon,\tau[$, for any $\varepsilon\in]0,\tau[$. Hence, if φ_1 is continuously differentiable, we can write

$$\begin{aligned}
\int_0^{\tau-\varepsilon}\frac{\partial F_1}{\partial\tau}(z,\tau-\lambda)\varphi_1(\lambda)d\lambda &= -\int_0^{\tau-\varepsilon}\frac{\partial F_1}{\partial\lambda}(z,\tau-\lambda)\varphi_1(\lambda)d\lambda\\
&= F_1(z,\tau)\varphi_1(0) - F_1(z,\varepsilon)\varphi_1(\tau-\varepsilon)\\
&\quad + \int_0^{\tau-\varepsilon}F_1(z,\tau-\lambda)\dot{\varphi}_1(\lambda)d\lambda
\end{aligned}$$

for every $z \in]0,1[, \tau > 0$ and $\varepsilon \in]0,\tau[$. Letting $\varepsilon \to 0$, and noting that $F_1(z,0) = 0$, we get

$$\int_0^\tau \frac{\partial F_1}{\partial \tau}(z,\tau-\lambda)\varphi_1(\lambda)d\lambda = F_1(z,\tau)\varphi_1(0) + \int_0^\tau F_1(z,\tau-\lambda)\dot{\varphi}_1(\lambda)d\lambda \tag{25}$$

We first consider the case $\varphi_1(0) = 0$. The above identity and Eq. (18) give

$$\xi(z,\tau) = (1-z)\varphi_1(\tau) - \frac{2}{\pi}\int_0^\tau \sum_{n=1}^{\infty} \frac{1}{n}\sin(n\pi z)e^{-n^2\pi^2(\tau-\lambda)}\dot{\varphi}_1(\lambda)d\lambda \tag{26}$$

If φ_1 is twice differentiable, we integrate by parts once more, and we find

$$\begin{aligned}\xi(z,\tau) &= (1-z)\varphi_1(\tau) - \frac{2}{\pi^3}\sum_{n=1}^{\infty}\frac{1}{n^3}\sin(n\pi z)\dot{\varphi}_1(\tau)\\ &+ \frac{2}{\pi^3}\sum_{n=1}^{\infty}\frac{1}{n^3}\sin(n\pi z)e^{-n^2\pi^2\tau}\dot{\varphi}_1(0)\\ &+ \frac{2}{\pi^3}\int_0^\tau\sum_{n=1}^{\infty}\frac{1}{n^3}\sin(n\pi z)e^{-n^2\pi^2(\tau-\lambda)}\ddot{\varphi}_1(\lambda)d\lambda\end{aligned} \tag{27}$$

After the second integration by parts, the series that define ξ in Eq. (27) converge uniformly, and we can interchange integration and summation.

Analogously, if φ_2 is twice continuously differentiable, we get the following solution to Eq. (20):

$$\begin{aligned}\chi(z,\tau) &= z\varphi_2(\tau) - \frac{2}{\pi^3}\sum_{n=1}^{\infty}\frac{(-1)^{n+1}}{n^3}\sin(n\pi z)\dot{\varphi}_2(\tau)\\ &+ \frac{2}{\pi^3}\sum_{n=1}^{\infty}\frac{(-1)^{n+1}}{n^3}\sin(n\pi z)e^{-n^2\pi^2\tau}\dot{\varphi}_2(0)\\ &+ \frac{2}{\pi^3}\int_0^\tau\sum_{n=1}^{\infty}\frac{(-1)^{n+1}}{n^3}\sin(n\pi z)e^{-n^2\pi^2(\tau-\lambda)}\ddot{\varphi}_2(\lambda)d\lambda\end{aligned} \tag{28}$$

Considering Eqs. (10), (27), and (28), we set

$$\begin{aligned}\vartheta_N(z,\tau) &= 2\sum_{n=1}^{N}e^{-n^2\pi^2\tau}\sin(n\pi z)\int_0^1\psi(y)\sin(n\pi y)dy\\ &+[(1-z)\varphi_1(\tau)+z\varphi_2(\tau)]\\ &-\frac{2}{\pi^3}\sum_{n=1}^{N}\frac{1}{n^3}\sin(n\pi z)[\dot{\varphi}_1(\tau)+(-1)^{n+1}\dot{\varphi}_2(\tau)]\\ &+\frac{2}{\pi^3}\sum_{n=1}^{N}\frac{1}{n^3}\sin(n\pi z)e^{-n^2\pi^2\tau}[\dot{\varphi}_1(0)+(-1)^{n+1}\dot{\varphi}_2(0)]\\ &+\frac{2}{\pi^3}\int_0^\tau\sum_{n=1}^{N}\frac{1}{n^3}\sin(n\pi z)e^{n^2\pi^2(\lambda-\tau)}[\ddot{\varphi}_1(\lambda)+(-1)^{n+1}\ddot{\varphi}_2(\lambda)]d\lambda\end{aligned} \tag{29}$$

and we note that $\vartheta(z,\tau) = \lim_{N\to\infty}\vartheta_N(z,\tau)$ is the solution to problem (3)–(4).

Figure 2(*b*) shows the solution to problem (3) with boundary conditions (24), as given by Eq. (29). Note that the oscillations highlighted in Fig. 2(*a*) now disappear. The quality of the solution is improved by the good rate of convergence of the series in Eqs. (10), (27), and (28).

Indeed, if the functions φ_1, φ_2, and ψ are bounded with their first and second derivatives on the interval [0, s], then we have

$$\max_{(z,\tau)\in[0,1]\times[0,s]}|\vartheta(z,\tau) - \vartheta_N(z,\tau)| \le \frac{C_s}{N^2} \tag{30}$$

for some positive constant C_s only depending on $\varphi_1, \varphi_2, \psi$, and s. This statement directly follows from the elementary inequality

$$\sum_{n=N+1}^{\infty}\frac{1}{n^3} \le \int_N^\infty \frac{1}{y^3}dy = \frac{1}{2N^2}$$

As a consequence, we also get the following stability estimate:

$$\|\vartheta_N(z,\tau)\|_{L^\infty([0,1]\times[0,s])} \le C_s \tag{31}$$

with the same constant C_s appearing in Eq. (30).

In conclusion, the regularity of the boundary and initial data improves the convergence of the numerical approximations. This remark agrees with the results provided by Surana et al. [7], where it is shown that finite element methods are even more sensitive to the regularity of the boundary data.

It is important to point out, however, that if we remove the assumption $\varphi_1(0) = \varphi_2(0) = 0$, we need to add the term $F_1(z,\tau)\varphi_1(0) + F_2(z,\tau)\varphi_2(0)$ in the definition of $\vartheta(z,\tau)$. Note that F_1 and F_2 are discontinuous at $(z,\tau) = (0,0)$ and $(z,\tau) = (1,0)$, respectively, then the convergence of series (18) is not uniform, and an approximation of $F_1(z,\tau)$ and $F_2(z,\tau)$ based on Eq. (18) cannot preserve the convergence rate (30). The alternative method introduced in next section will overcome the above difficulty.

5 An Alternative Approach

In this section, we rely on another classical method, based on the Laplace transform, (see for instance Ref. [3]) that gives a different expression of the function F_1 appearing in Eq. (15). To avoid ambiguities, we will denote such expression by $\widetilde{F}_1$

$$\widetilde{F}_1(z,\tau) = \sum_{n=0}^{\infty}\left[\mathrm{erfc}\left(\frac{2n+z}{2\sqrt{\tau}}\right) - \mathrm{erfc}\left(\frac{2(n+1)-z}{2\sqrt{\tau}}\right)\right] \tag{32}$$

Here, erfc is the complementary error function

$$\mathrm{erfc}(z) = \frac{2}{\sqrt{\pi}}\int_z^{+\infty} e^{-y^2}dy \quad z \in \mathbf{R}$$

A good feature of series (32) is that the discontinuity in F_1 does not affect its uniform convergence. Indeed

$$g(z,\tau) = \frac{z}{2\sqrt{\tau}}$$

is the Green's function of the half line $\{(z<1)\}$ and is discontinuous at $(z,\tau) = (0,0)$, while $\widetilde{F}_1 - g$ is continuous at $(z,\tau) = (0,0)$. It is immediate to show that Eq. (32) has an excellent rate of convergence. In fact, for any given positive s, we have

$$\begin{aligned}\sum_{n=0}^{\infty}\sup_{(z,\tau)\in[0,1]\times[0,s]}&\left|\mathrm{erfc}\left(\frac{2n+z}{2\sqrt{\tau}}\right) - \mathrm{erfc}\left(\frac{2(n+1)-z}{2\sqrt{\tau}}\right)\right|\\ &\le \sum_{n=0}^{\infty}\mathrm{erfc}\left(\frac{n}{\sqrt{s}}\right)\end{aligned} \tag{33}$$

where the convergence of the right-hand side term is very fast. Hence, if ξ denotes the solution of Eq. (8), by Eqs. (15) and (25), we get

$$\xi(z,\tau) = \int_0^\tau \dot{\varphi}_1(\lambda)\sum_{n=0}^{\infty}\left[\mathrm{erfc}\left(\frac{2n+z}{2\sqrt{\tau-\lambda}}\right) - \mathrm{erfc}\left(\frac{2(n+1)-z}{2\sqrt{\tau-\lambda}}\right)\right]d\lambda$$

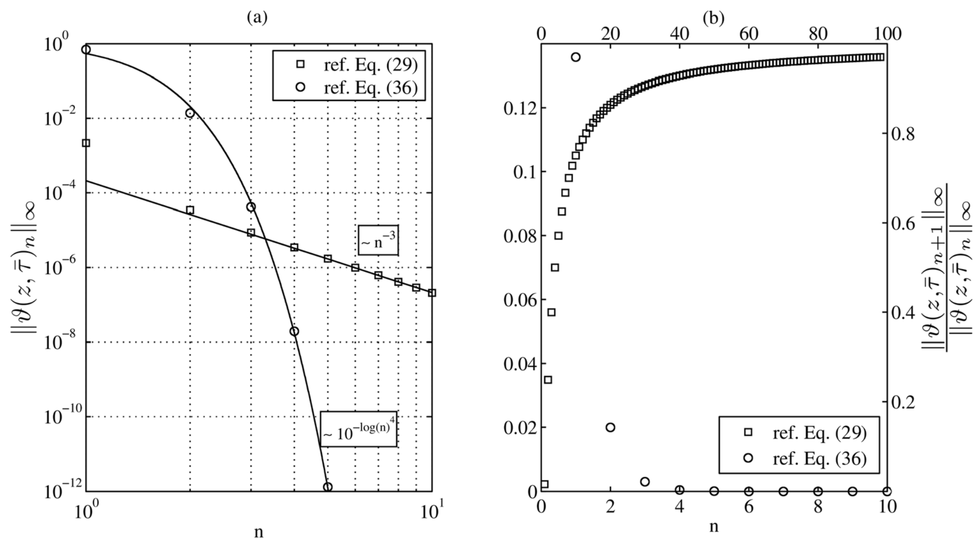

Fig. 3 Numerical assessment of convergence rates: (*a*) infinity norm of the *n*-th series terms and (*b*) ratio between the norms of successive terms versus *n* in Eqs. (29) and (36)

Here, F_1 has been replaced by $\widetilde{F}_1$. The good rate of convergence of Eq. (32) allows us to remove the assumption $\varphi_1(0) = 0$. We get

$$\xi(z,\tau) = \varphi_1(0)\sum_{n=0}^{\infty}\left[\operatorname{erfc}\left(\frac{2n+z}{2\sqrt{\tau-\lambda}}\right) - \operatorname{erfc}\left(\frac{2(n+1)-z}{2\sqrt{\tau-\lambda}}\right)\right] + \int_0^{\tau}\dot{\varphi}_1(\lambda)\sum_{n=0}^{\infty}\left[\operatorname{erfc}\left(\frac{2n+z}{2\sqrt{\tau-\lambda}}\right) - \operatorname{erfc}\left(\frac{2(n+1)-z}{2\sqrt{\tau-\lambda}}\right)\right]d\lambda \tag{34}$$

Analogously, the solution χ to problem (9) writes

$$\chi(z,\tau) = \int_0^{\tau}\left[\varphi_2(\lambda)\frac{\partial\widetilde{F}_2(z,\tau-\lambda)}{\partial\tau}\right]d\lambda$$

where $\widetilde{F}_2(z,\tau) = \widetilde{F}_1(1-z,\tau)$, so that

$$\chi(z,\tau) = \varphi_2(0)\widetilde{F}_2(z,\tau) + \int_0^{\tau}\dot{\varphi}_2(\lambda)\widetilde{F}_2(z,\tau-\lambda)d\lambda \tag{35}$$

From Eqs. (10), (34), and (35) we deduce a novel expression of ϑ_N, in the form

$$\begin{aligned}\vartheta_N(z,\tau) = {} & \varphi_1(0)\sum_{n=0}^{N}\left[\operatorname{erfc}\left(\frac{2n+z}{2\sqrt{\tau}}\right) - \operatorname{erfc}\left(\frac{(2n+2)-z}{2\sqrt{\tau}}\right)\right] \\ & + \varphi_2(0)\sum_{n=0}^{N}\left[\operatorname{erfc}\left(\frac{(2n+1)-z}{2\sqrt{\tau}}\right) - \operatorname{erfc}\left(\frac{(2n+1)+z}{2\sqrt{\tau}}\right)\right] \\ & + \int_0^{\tau}\dot{\varphi}_1(\lambda)\sum_{n=0}^{N}\left[\operatorname{erfc}\left(\frac{2n+z}{2\sqrt{\tau-\lambda}}\right) - \operatorname{erfc}\left(\frac{(2n+2)-z}{2\sqrt{\tau-\lambda}}\right)\right]d\lambda \\ & + \int_0^{\tau}\dot{\varphi}_2(\lambda)\sum_{n=0}^{N}\left[\operatorname{erfc}\left(\frac{(2n+1)-z}{2\sqrt{\tau-\lambda}}\right) - \operatorname{erfc}\left(\frac{(2n+1)+z}{2\sqrt{\tau-\lambda}}\right)\right]d\lambda \\ & + 2\sum_{n=1}^{N}e^{-n^2\pi^2\tau}\sin(n\pi z)\int_0^1\psi(y)\sin(n\pi y)dy\end{aligned} \tag{36}$$

The numerical method based on the above approximation remains numerically stable and maintains a very fast convergence even if the boundary data are discontinuous. The convergence properties of the function ϑ_N defined in Eq. (36) entail the result of Fig. 2(*c*), where the solution to problem (3) with boundary conditions (24) is shown, as computed by Eq. (36). The shape of the solution is perfectly identical to that displayed in Fig. 2(*b*), highlighting that the two expressions (29) and (36) lead to substantially equivalent results.

As already stated, the difference between the two approaches lies in the faster convergence of Eq. (36) with respect to Eq. (29). This is consequential to the fact that Eq. (19) involves the Fourier series of a discontinuous function, and its convergence rate is slower than the one of the series appearing in Eqs. (34) and (35).

The above assertion can easily be demonstrated by computing some norm of the *n*-th term of the series appearing in Eqs. (29) and (36), $\vartheta_n(z,\tau)$, and by evaluating its value for increasing *n*. As an example, by taking problem (3) with boundary conditions (24), we evaluated the infinity norm of $\vartheta_n(z,\bar{\tau})$, for $\bar{\tau} = 1$ with both approaches, and plotted it as a function of *n*. The result is shown in Fig. 3(*a*). From the graphs it appears clearly that the magnitude of terms in solution (29) decreases by a power law ($\sim n^{-3}$), whilst the rate of decay of the terms in solution (36) is exponential and, therefore, much faster. For both solutions, Table 1 reports the value of *n* for which $\vartheta_n(z,\bar{\tau})$ falls below selected thresholds, thus providing a useful indication for the application of the formulas (29) and (36) whenever a numerical evaluation of the solution to a problem of the kind (3)–(4) is sought for.

Figure 3(*b*) reports the trends of the ratio R_ϑ

$$R_\vartheta = \frac{\|\vartheta(z,\bar{\tau})_{n+1}\|_\infty}{\|\vartheta(z,\bar{\tau})_n\|_\infty}$$

for increasing *n*. We note that R_ϑ tends to a finite limit in the interval]0,1[for the solution obtained by Eq. (29), suggesting that the convergence of the series is linear. On the other hand, R_ϑ goes rapidly to 0 for the solution obtained by Eq. (36), proving that the series has superlinear convergence.

Table 1 Number of terms in Eqs. (29) and (36) after which the infinity norm of the *n*-th term falls below a given threshold

Threshold	Eq. (29)	Eq. (36)
10^{-6}	$n=6$	$n=4$
10^{-8}	$n=27$	$n=5$
10^{-10}	$n=60$	$n=5$

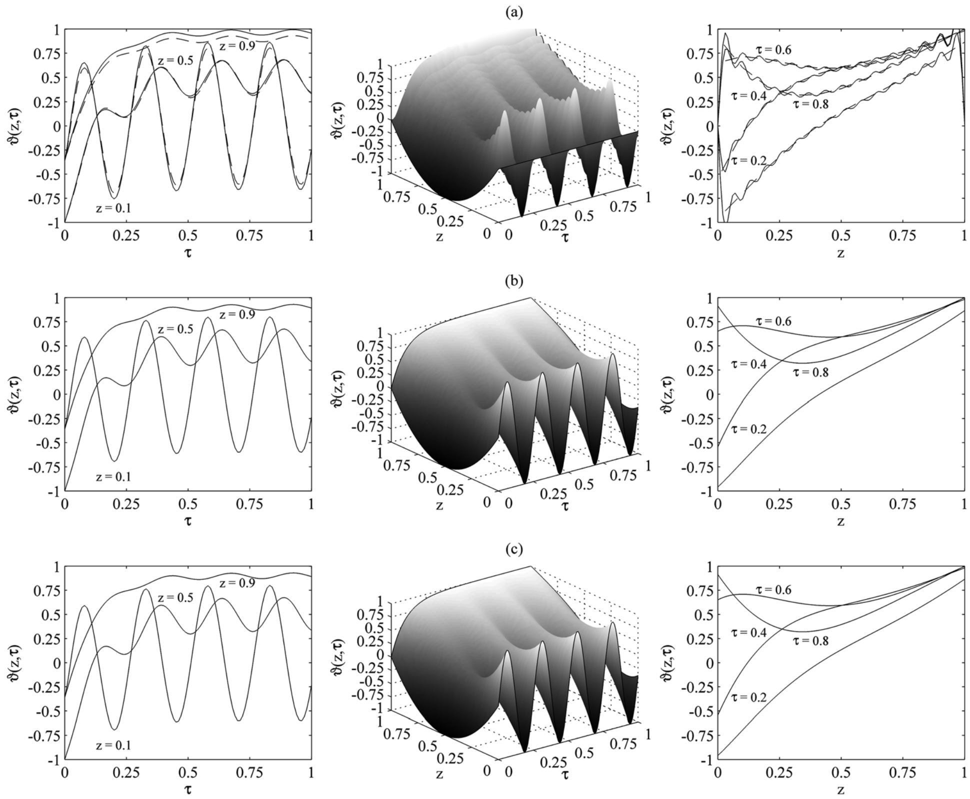

Fig. 4 Solutions to Eq. (3) with boundary conditions (37), computed on the $[0,1]\times[0,1]$ domain according to: (*a*) Eq. (22); (*b*) Eq. (29); (*c*) Eq. (36). All the finite sums are evaluated up to a number of terms $N=30$. Left panels: profiles of $\vartheta(z,\tau)$ for selected *z*-values. Middle panels: surface visualization of $\vartheta(z,\tau)$. Right panels: profiles of $\vartheta(z,\tau)$ for selected τ-values. Dashed lines in left and right panels denote a numerical solution obtained by second-order finite differencing.

In a similar fashion to Fig. 2, numerical solutions to problem (3), for the following set of initial and boundary conditions:

$$\begin{aligned}
\vartheta(z,0) &= \psi(z) := 4z^2 - 4z, \qquad 0 \le z \le 1\\
\vartheta(0,\tau) &= \varphi_1(\tau) := 1 - e^{-10\tau}, \qquad \tau \ge 0\\
\vartheta(1,\tau) &= \varphi_2(\tau) := \sin(25\tau), \qquad \tau \ge 0
\end{aligned} \tag{37}$$

are reported in Fig. 4, according to Eqs. (*a*) (22), (*b*) (29), and (*c*) (36). Being this a more general case than the example given by Eq. (24), it confirms the qualities of the two solution methods proposed here. It also highlights the suitability of the two approaches to problems with oscillating boundary values.

6 Concluding Remarks

Analytical solutions to the one-dimensional heat equation were considered for time-varying Dirichlet-type boundary conditions and arbitrary initial values.

Standard approaches in the literature, based on Green representation formulas and the Duhamel's integral, were shown to have poor convergence rates and to provide inaccurate results, in particular when discontinuities are present at the boundaries, or the imposed boundary values oscillate in time.

More accurate and uniformly convergent solutions were obtained following two alternative approaches. The first solution was derived by double integration by parts starting from the classical Fourier expansions. The second procedure enforced the Duhamel's integral coupled with the Laplace transform.

We gave a rigorous theoretical estimate of the rate of convergence of the series that define the two solutions, and we showed that they both converge uniformly on the domain. In addition, we demonstrated that the second solution maintains its validity even in the presence of a finite number of discontinuities in the boundary functions.

A numerical estimate of the convergence rate of the two solutions was provided for two test cases, showing that both methods have superior accuracy and convergence properties towards the standard approach. The numerical experiments also indicated that the second method has a higher convergence rate than the first one, thus representing a very attractive computational tool for direct use or the benchmarking of numerical discretizations.

Nomenclature

C = constant
f, g = auxiliary functions
$F_1, \widetilde{F}_1, F_2, \widetilde{F}_2$ = auxiliary functions for the Duhamel's integral
G = Green's functions
R_ϑ = ratio of the norms of successive series terms
t = time (*s*)
T_0 = initial temperature distribution
T_1 = boundary temperature values at $z=0$
T_2 = boundary temperature values at $z=1$
s = arbitrary scalar
x = space coordinate (*m*)
y = auxiliary integration variable
z = dimensionless space variable

Greek Symbols

α = thermal diffusivity
ϑ = dimensionless temperature
λ = auxiliary integration variable

$\tau =$ dimensionless time
$\varphi_1 =$ dimensionless boundary condition at $z = 0$
$\varphi_2 =$ dimensionless boundary condition at $z = 1$
$\xi, \eta, \rho, \chi =$ auxiliary functions
$\psi =$ dimensionless initial condition

References

[1] Carslaw, H. S., and Jaeger, J. C., 1959, *Conduction of Heat in Solids*, 2nd ed., Oxford University, London, UK.
[2] Arpaci, V. S., 1966, *Conduction Heat Transfer*, Addison-Wesley, Reading, MA.
[3] Ozisik, M. N., 1968, *Boundary Value Problems of Heat Conduction*, International Textbook, Scranton, PA.
[4] Ozisik, M. N., 1980, *Heat Conduction*, John Wiley and Sons, New York.
[5] Schuh, H., 1965, *Heat Transfer in Structures* (International Series of Monographs in Aeronautics and Astronautics), Pergamon, Oxford, UK.
[6] Ozisik, M. N., 1985, *Heat Transfer, A Basic Approach*, McGraw-Hill Book Company, New York.
[7] Surana, K. N., Reddy, J. N., and Allu, S., 2007, "The k-Version of Finite Element Method for Initial Value Problems: Mathematical and Computational Framework," Int. J. Comput. Methods Eng. Sci. Mech., **8**, pp. 123–136.
[8] Surana, K. N., Ma, Y., Romkes, A., and Reddy, J. N., 2010, "Development of Mathematical Models and Computational Framework for Multi-Physics Interaction Processes," Mech. Adv. Mater. Struct., **17**, pp. 488–508.
[9] Poletkin, K. V., and Kulish, V., 2012, "Steady State Heat Transfer Within a Nanoscale Spatial Domain," ASME J. Heat Transfer, **134**, p. 074503.
[10] Alassar, R. J., 2012, "Transient Conduction From Parallel Isothermal Cylinders," J. Heat Transfer, **134**, p. 121301.
[11] Di Benedetto, E., 1995, *Partial Differential Equations*, Birkauser, Boston, MA.
[12] Pini, B., 1994, *Terzo Corso di Analisi Matematica*, Clueb editori, Bologna, Italy, Chap. 1.